Chapter

The Effect of Random Load on Life Prediction of High-Temperature Ceramic Matrix Composites

En-Zhong Zhang

Abstract

High-temperature ceramic matrix composites (CMCs) are widely used in hot section components of aeroengine, and random loads have an important effect on their safety and reliability during aircraft operation. The current fatigue life prediction model of CMC is divided into macrophenomenon model and microdamage mechanism model. In this chapter, the fatigue life of fiber-reinforced ceramic matrix composites is investigated. The fatigue life of the fiber-reinforced ceramic matrix composites is predicted by micromechanical methods. The effect of random loading on fatigue life is analyzed and compared with constant peak stress fatigue life. The influence of composite constitutive properties on fatigue fracture is also discussed.

Keywords: high-temperature ceramic matrix composites, fatigue life, random load, fiber failure

1. Introduction

In the rapid progress and development of science and technology, the requirements of the use environment of the required materials are also increasing. For example, with the development of high-performance aero-turbine engine, the inlet temperature of the turbine increases gradually, and the temperature of the hot-end parts can reach more than 1600°C, which has far exceeded the working limit of superalloy [1]. The main materials of aeroengine combustion chamber, turbine, and other high-temperature structures are still superalloys, although cooling and thermal barrier coating technology is developing, but still cannot fully meet the requirements of engine hot-end components, so high-temperature ceramic-based composites are born. Ceramic matrix composites (CMCs) have a great potential as high-temperature structural materials, especially as materials used in aerospace vehicles with special parts which need to bear a very high temperature.

Compared with traditional materials, ceramic matrix composites have the advantages of wear resistance, high temperature resistance, chemical corrosion resistance, good vibration absorption, high specific strength, high specific modulus, and low cost. The density is only 1/4–1/3 of the nickel-base alloy, and the strength will not decrease with the increase of temperature, even higher than at room temperature. The application of ceramic matrix composite material structure to civil engine can reduce the amount of cooling air, increase the temperature and efficiency before turbine, and reduce the fuel consumption rate, so it can improve the economy of the engine. If the ceramic matrix composite structure is applied to the military engine, the starting weight can be obviously reduced, the temperature in front of the turbine can be increased, and the pushing weight ratio of the engine can be improved.

The most successful engine company for SiC_f/ SiC composite is the GE Aviation Group. The GE Aviation Group, supported by the US Department of Energy project, in 1992 developed innovative prepreg-melt infiltration processes that allow high-performance, rapid, and low-cost preparation of SiC_f/SiC composites becomes a reality. Developed by the GE Aviation Group, the SiC_f/ SiC composite low-pressure guide vane was verified on the F136 engine in 2009, and the first flight was completed in 2010. In 2016, SiC_f/SiC composite is applied on the turbine outer ring of Leading Edge Aviation Propulsion (LEAP) engines and produced in batches. The SiC_f/ SiC composite is used in combustor, guide vane, and turbine outer ring of GE9X commercial engine, which reduces fuel consumption by 10% compared with GE90-115B engine. The new generation of military turboshaft GE3000 engine uses a ceramic matrix composite material, which reduces fuel consumption by 25% compared with T700 engine, reduces life cycle cost by 35%, prolongs life by 20%, and increases work-weight ratio by 65%. The Safran Group is one of the leading practitioners of SiC_f/SiC ceramic matrix composites; the company has mastered the chemical vapor infiltration process and has taken the lead in applying it on engine tail nozzle.

There are two kinds of fatigue life prediction models for ceramic matrix composites, i.e., macroscopic phenomenological model [2] and micromechanical damage mechanism model [3]. Due to the complex microstructure, high anisotropy, and various damage mechanisms of ceramic matrix composites, the macroscopic phenomenological model needs a lot of experimental data to modify the life model. The influence of structure fatigue life of high-temperature ceramic matrix composites is closely related to the reliability and safety of aircraft; it is necessary to investigate the influence of random load on structure fatigue life of high-temperature ceramic matrix composites.

In this chapter, the damage process and mechanism of ceramic matrix composites are studied by means of the micromechanical method. The influence of random load on fatigue life prediction of high-temperature ceramic matrix composites is studied. According to the fatigue fracture mechanism of composite under cyclic load, the life prediction model of composite is established, and an external load is applied to study the influence of random load on fatigue life prediction of high-temperature ceramic matrix composites.

2. Prediction method of fatigue life of composite materials

Fatigue damage occurs in composites subjected to repeated loading. Fatigue damage at the initial stage of material application is not easily detected in external observation. With the increasing number of cycles, the matrix began to appear cracks, interfacial debonding, delamination, and irreversible fatigue damage. Results show that the interfacial shear stress and fiber strength will decrease with the increasing number of cycles. The decrease of interfacial shear stress causes the material to be unable to deliver the load effectively, and the fiber strength is reduced, resulting in the material being difficult to resist deformation. With their combined action, the fiber volume failure percentage increases with the increasing number of cycles. When the fiber volume failure percentage increases to a critical value, the composite will be damaged. Under critical conditions, with the increase of fatigue peak stress, it will lead to the decrease of cycle times, the decrease of lifetime, and the decrease of safety and reliability.

Li [4] developed a micromechanical fatigue life prediction model considering interface wear and fiber failure. In the process of cyclic loading to fatigue peak load, some fibers first break failure, but also can bear a certain load through interfacial shear stress. The load distribution between an intact fiber and a broken fiber is as follows:

$$\frac{\sigma_{\max}}{V_f} = T[1 - P(T)] + < T_b > P(T) \tag{1}$$

where σ_{max} is the fatigue peak stress, V_f is the fiber volume content, $<T_b>$ is the load carried by the broken fiber, and P(T) is the fiber failure probability:

$$P(T) = 1 - \exp\left\{ -\left(\frac{T}{\sigma_c}\right)^{m+1} \left(\frac{\sigma_0}{\sigma_0(N)}\right)^m \left(\frac{\tau_i}{\tau_i(N)}\right) \right\} \tag{2}$$

where σ_c is the characteristic strength of the reinforced fiber and m is the fiber Weibull modulus.

Lee [5] investigated the tension-tension fatigue behavior of CMCs at room temperature; the degradation of the fiber strength is

$$\sigma_0(N) = \sigma_0\left[1 - p_1(\log N)^{p_2}\right] \tag{3}$$

where p_1 and p_2 are the empirical parameters.

Evans et al. [6] investigated the fatigue behavior of SiC/CAS composite at room temperature. The degradation of the interfacial shear stress is

$$\tau_i(N) = \tau_{i0} + \left[1 - \exp\left(-\varpi N^{\lambda}\right)\right](\tau_{i\min} - \tau_{i0}) \tag{4}$$

where τ_{i0} is the initial value of the interfacial shear stress, $\tau_{i\ min}$ is the steady-state value of interfacial shear stress, and ω and λ are the empirical parameters.

Substituting the stress carried by broken fiber into Eq. (1), it leads to

$$\frac{\sigma_{\max}}{V_f} = T\left(\frac{\sigma_0(N)}{\sigma_0}\right)^m \left(\frac{\sigma_c}{T}\right)^{m+1} \frac{\tau_i(N)}{\tau_i} \left\{1 - \exp\left[-\left(\frac{T}{\sigma_c}\right)^{m+1} \left(\frac{\sigma_0}{\sigma_0(N)}\right)^m \frac{\tau_i}{\tau_i(N)}\right]\right\} \tag{5}$$

Using Eqs. (3), (4), and (5), the intact fiber stress T can be obtained N the change of cycle number

$$\begin{aligned}\frac{\sigma_{\max}}{V_f} = T\left\{\left[1 - P_1(\log N)^{P_2}\right]\right\}\left(\frac{\sigma_c}{T}\right)^{m+1} \frac{\tau_{i0} + \left[1 - \exp\left(-\varpi N^{\lambda}\right)\right](\tau_{i\min} - \tau_{i0})}{\tau_i} \\ \cdot\left\{1 - \exp\left[-\left(\frac{T}{\sigma_c}\right)^{m+1}\left(\frac{1}{1 - P_1(\log N)^{P_2}}\right)^m \frac{\tau_i}{\tau_{i0} + \left[1 - \exp\left(-\varpi N^{\lambda}\right)\right](\tau_{i\min} - \tau_{i0})}\right]\right\}\end{aligned} \tag{6}$$

Using Eq. (2), Eq. (6) changes to

$$\frac{\sigma_{\max}}{V_f} = T\{[1 - P_1(\log N)^{P_2}]\}\left(\frac{\sigma_c}{T}\right)^{m+1} \frac{\tau_{i0} + [1 - \exp(-\varpi N^{\lambda})](\tau_{i\min} - \tau_{i0})}{\tau_i} P(T) \tag{7}$$

When the failure fiber volume fraction P(T) reaches the critical value q*, the composite fatigue fails. The flowchart for the life prediction of CMCs is given by the following (**Figure 1**):

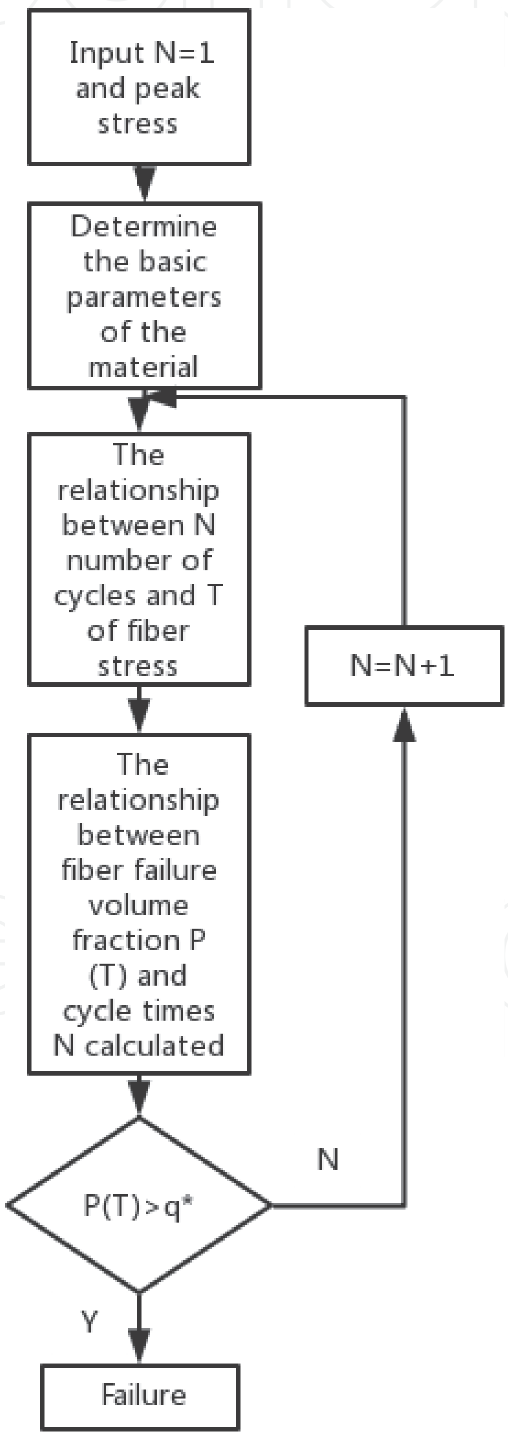

Figure 1.
The flowchart for life prediction of CMCs.

1. Determine the basic parameters of the material.

2. The relationship between the fiber strength and interfacial shear stress and cycle times N was calculated by Eqs. (3) and (4), respectively. Then, the relationship between an intact fiber stress T and cycle number N under a certain peak stress was calculated by Eq. (5).

3. The relationship between cycle number N and intact fiber stress T is obtained from Eq. (2), and the relationship between fiber failure fraction P (T) and cycle number is calculated by combining Eq. (7). When P (T) > q^*, the composite fails and the minimum cycle number is output N, which is fatigue life.

2.1 Theoretical prediction of ceramic matrix composites without random loading

For C/SiC composite, the model parameters are given by p_1 = 0.01 and p_2 = 1.0; the interfacial shear stress parameters are ω = 0.04, λ = 1.5, τ_{i0} = 8 MPa, and τ_{imin} = 0.3 MPa; and the other parameters are V_f = 0.42, σ_c = 2 GPa, m = 5, and τ_i = 10 MPa.

Figure 2 is derived from Eq. (3). It can be concluded that the fiber strength shows a linear decline with the increasing number of cycles and decreases from the original 100% to about 94% of the original value when the number of cycles reaches N = 1,000,000.

Figure 3 is calculated from Eq. (4). The interfacial shear stress decreases rapidly in the first 20 cycles and decreases very slowly and almost negligible in the 20–1,000,000 cycles, which is approximately a straight line. It can be speculated that the interface shear stress almost does not change with the increase of cycle times after 1,000,000 cycles.

Figures 4–6 are obtained by combining Eqs. (6) and (7) under a peak stress of σ_{max} = 355, 365, and 375 MPa, respectively. The fiber failure fraction of CMCs changes most slowly with the increase of cycle number in cycles from N = 1 to N = 100. In the 100–3000 cycles, the fiber failure fraction changes most sharply

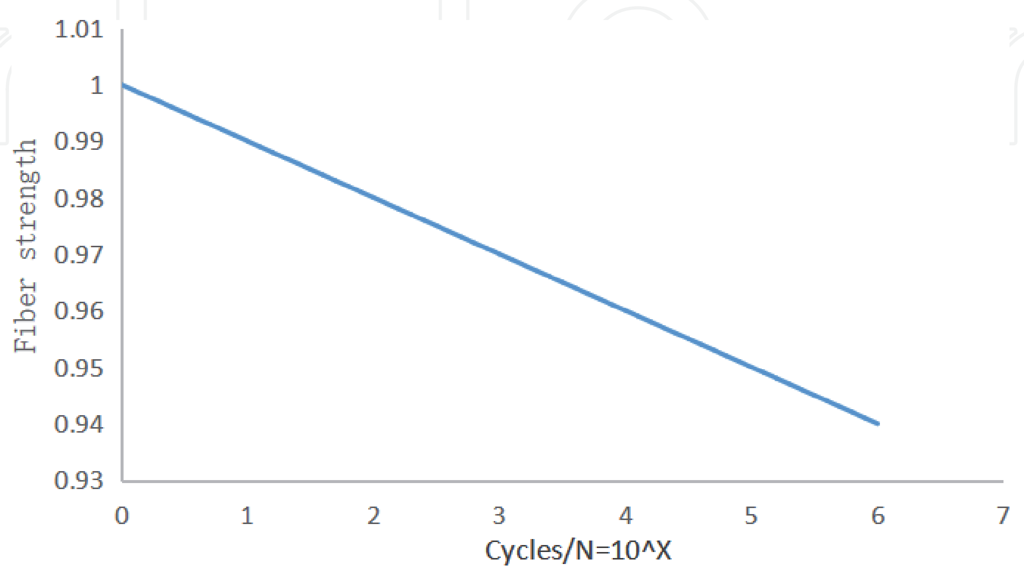

Figure 2.
Fiber strength versus cycle number curve.

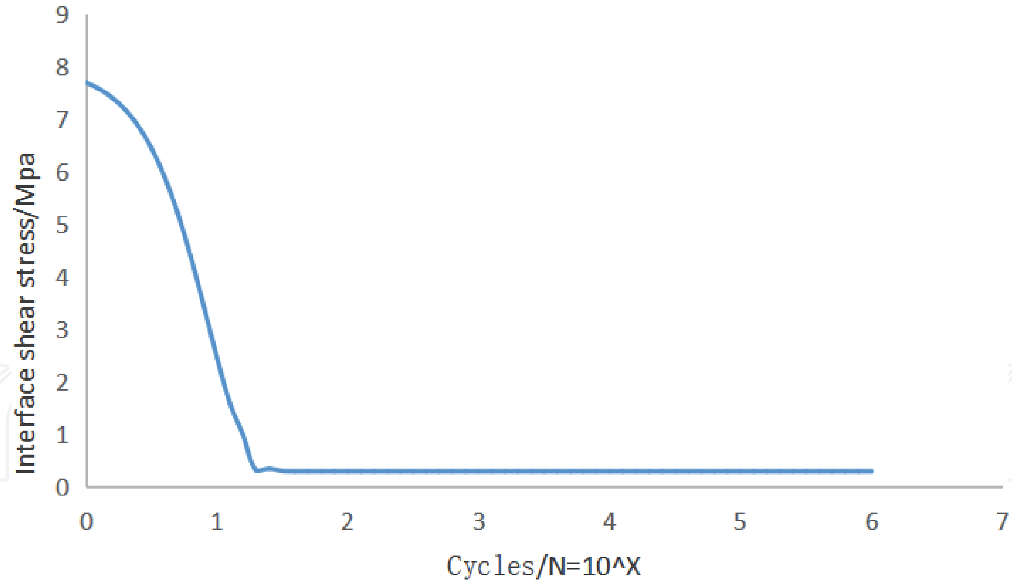

Figure 3.
Interfacial shear stress versus cyclic number curve.

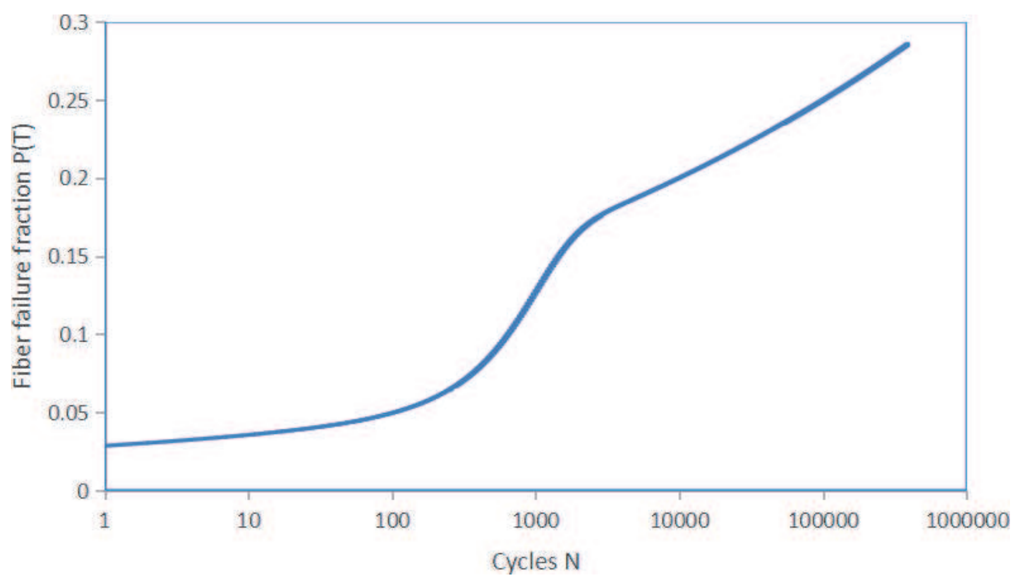

Figure 4.
Fiber failure fraction versus cycle number under $\sigma_{max} = 355$ *MPa.*

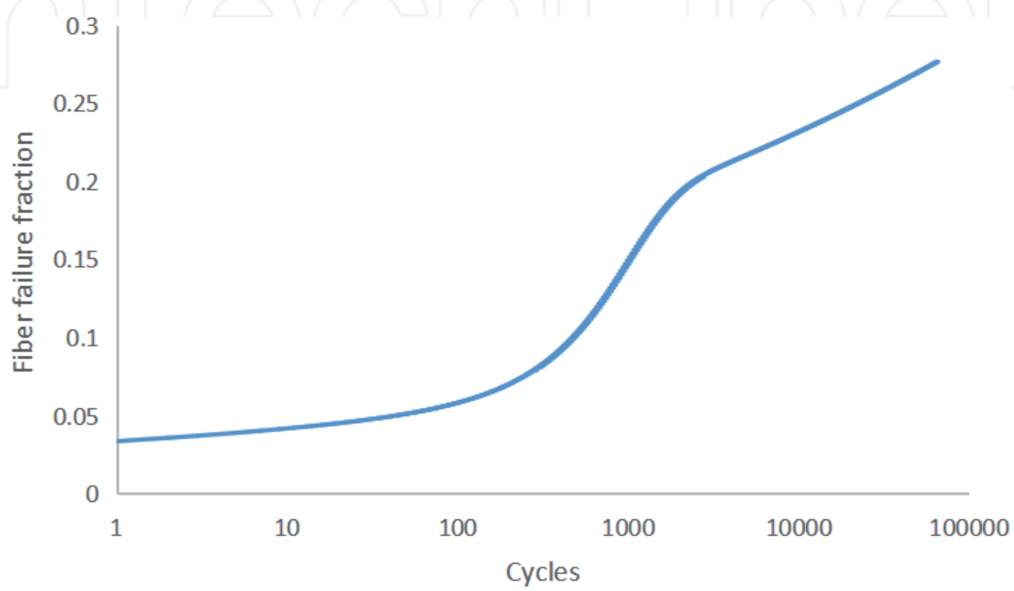

Figure 5.
Fiber failure fraction versus cycle number under $\sigma_{max} = 365$ *MPa.*

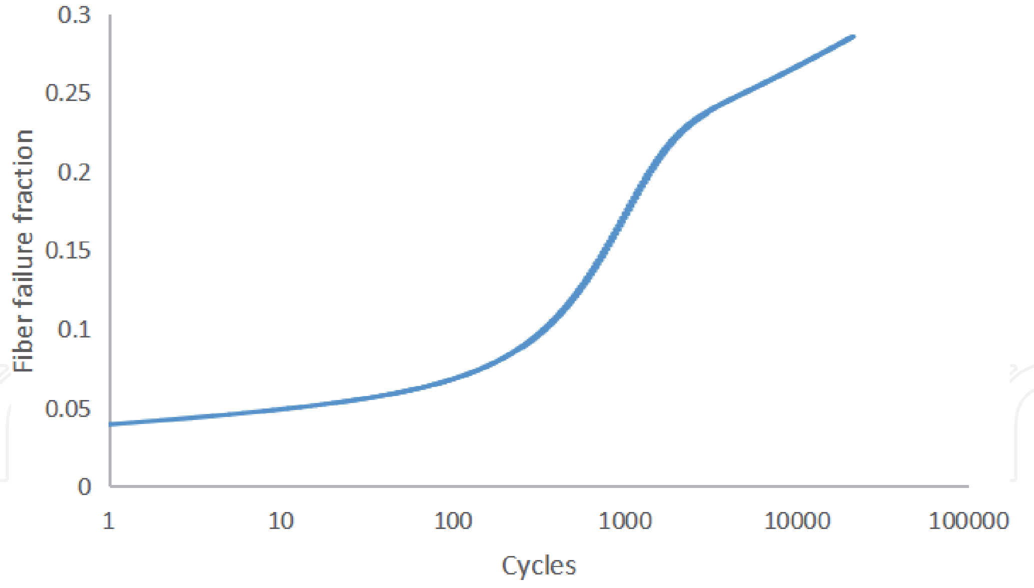

Figure 6.
Fiber failure fraction versus cycle number under σ_{max} *= 375 MPa.*

with the increase of cycle number. The fiber failure fraction in the cycles of 3000–1,000,000 is similar to the linear growth with the increase of the cycle number.

A calculation process of **Figure 7** can be obtained from the steps above. The S-N diagram of the composite is divided into segments. In the first cycle of 1–1000, the peak stress in the cycle changes very slowly in the increase of cycle number, which approximates a horizontal line. In the second stage, during the 1000–2000 cycles, the peak stress changes rapidly in the cycle number. In the third stage, in 2000–1,000,000, the peak stress in this cycle presents a linear decrease with the increase of the number of cycles.

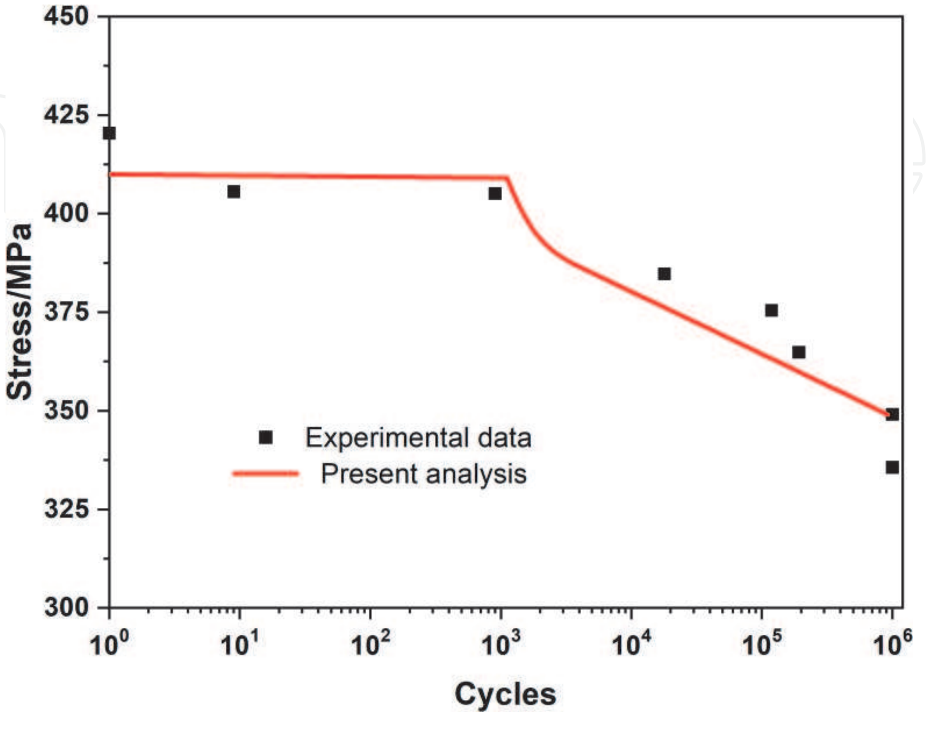

Figure 7.
The experimental and predicted S-N curve.

3. Effect of random load on fatigue life of ceramic matrix composites

The fiber characteristic strength and interfacial shear stress of CMCs are cyclic dependent. The addition of a random load at the Nth cycle can be considered to be the addition of a new peak stress higher than the original peak stress at the Nth cycle, which is approximately equivalent to cycling the random load as the constant peak stress, calculating the difference between its increased fiber failure probability at the Nth cycle relative to the fiber failure probability increased by the original peak stress at the Nth cycle k, and adding the k to the fiber failure rate after the first cycle.

3.1 Effect of random load cycle number on fatigue life

The parameters of C/SiC composite are given as follows: p_1 = 0.01 and p_2 = 1.0; the interfacial shear stress parameter is given by ω = 0.04, λ = 1.5, τ_{i0} = 8 MPa, and τ_{imin} = 0.3 MPa; the other related parameters are given by V_f = 0.42, σ_c = 2 GPa, m = 5, and τ_i = 10 MPa.

The fiber failure curves under a constant peak stress of σ_{max} = 355 MPa and random load of σ_s = 360 MPa at N = 100 are shown in **Figure 8**. At the 100th cycle, due to the random load of σ_s = 360 MPa, the fiber failure probability increases 0.004207 than the original value under σ_{max} = 355 MPa, the difference of fiber failure probability continues after 100 cycles, and the life is reduced from the original N = 389,642 cycles under σ_{max} = 355 MPa to N = 335,176 cycles, and the life difference is 54,466 cycles. The occurrence of random load reduces the fatigue life and decreases the fatigue life by 14.0% relative to the original value.

The fiber failure curves under a constant peak stress of σ_{max} = 355 MPa and random load of σ_s = 360 MPa at N = 1000 are shown in **Figure 9**. At the 100th cycle, due to the random load of σ_s = 360 MPa, the fiber failure probability increases 0.010321 than the original value under σ_{max} = 355 MPa, the difference of fiber failure probability continues after 1000 cycles, and the life is reduced from the original N = 389,642 cycles under σ_{max} = 355 MPa to N = 268,176 cycles, and the life difference is 121,466 cycles. The occurrence of random load reduces the fatigue life and decreases the fatigue life by 31.1% relative to the original value.

The fiber failure curves under a constant peak stress of σ_{max} = 355 MPa and random load of σ_s = 360 MPa at N = 10,000 are shown in **Figure 10**. At the 100th

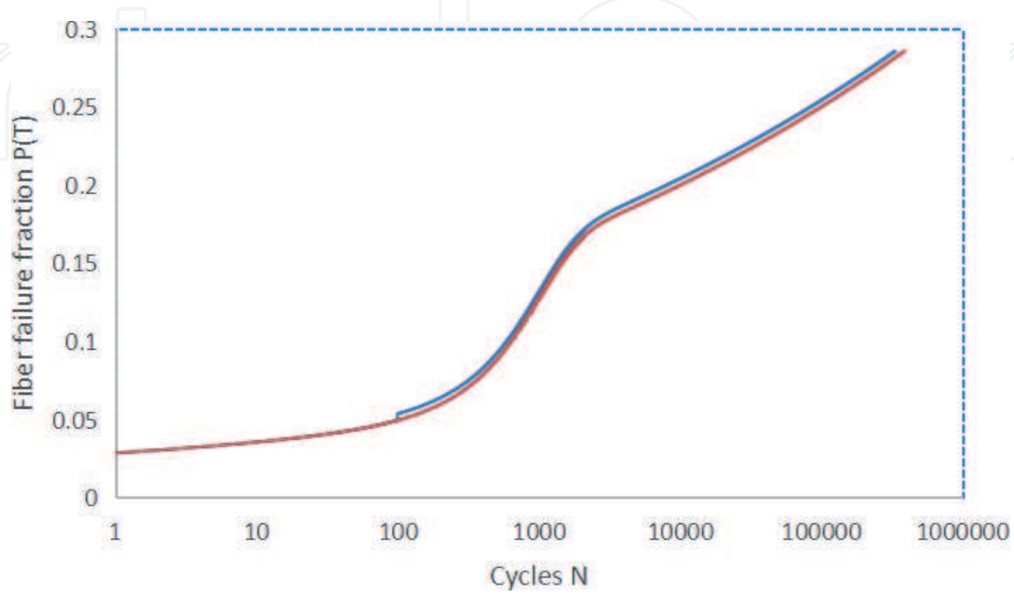

Figure 8.
The fiber failure probability versus cycle number under σ_{max} = 355 MPa and random load of σ_s = 360 MPa at N = 100.

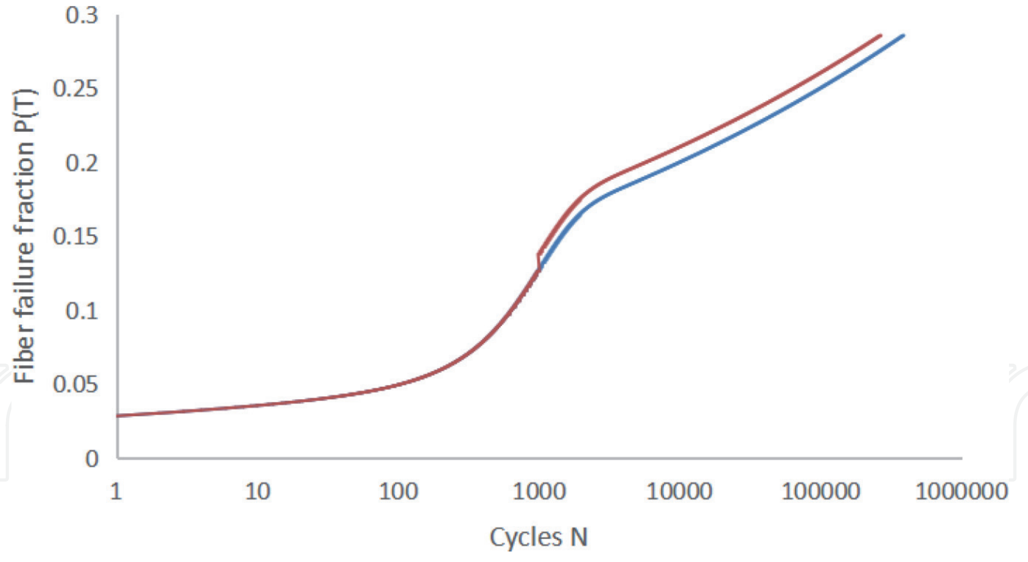

Figure 9.
The fiber failure probability versus cycle number under σ_{max} = 355 MPa and random load of σ_s = 360 MPa at N = 1000.

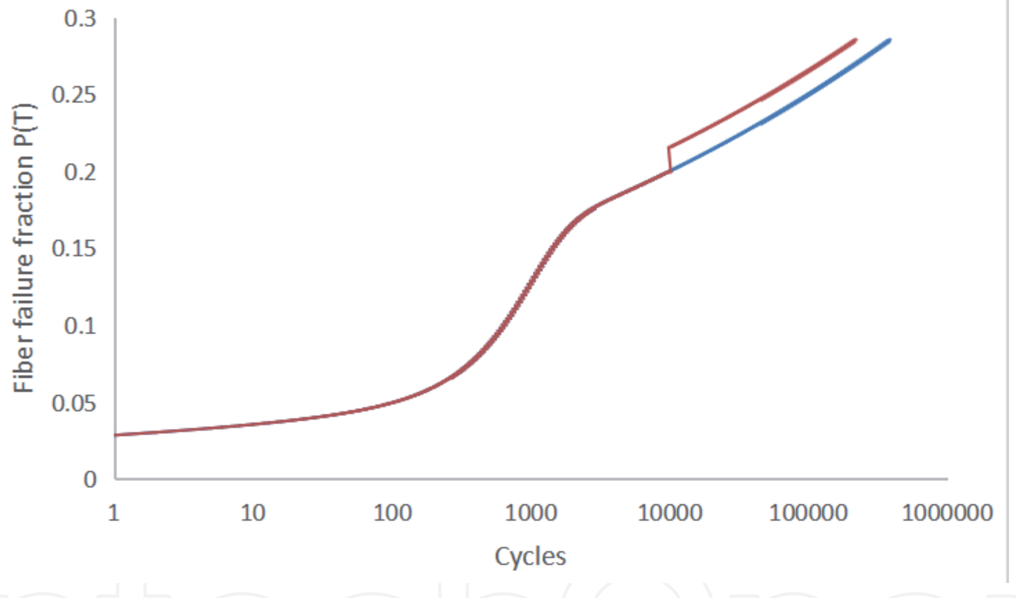

Figure 10.
The fiber failure probability versus cycle number under σ_{max} = 355 MPa and random load of σ_s = 360 MPa at N = 10,000.

Number of cycles	Fiber failure fraction under the original load	Fiber failure fraction after random load	Difference of fiber failure fraction	Fatigue life under original load	Fatigue life after random load	Difference of fatigue life	Fatigue life decreasing rate
100	0.049407	0.053614	0.004207	389,642	335,176	54,466	14.0%
1000	0.12704	0.137361	0.010321	389,642	268,176	121,466	31.1%
10,000	0.199833	0.215297	0.015464	389,642	221,415	168,227	43.2%

Table 1.
Fatigue life and fiber failure fraction under σ_{max} = 355 MPa and random load of σ_s = 360 MPa at different cycle number.

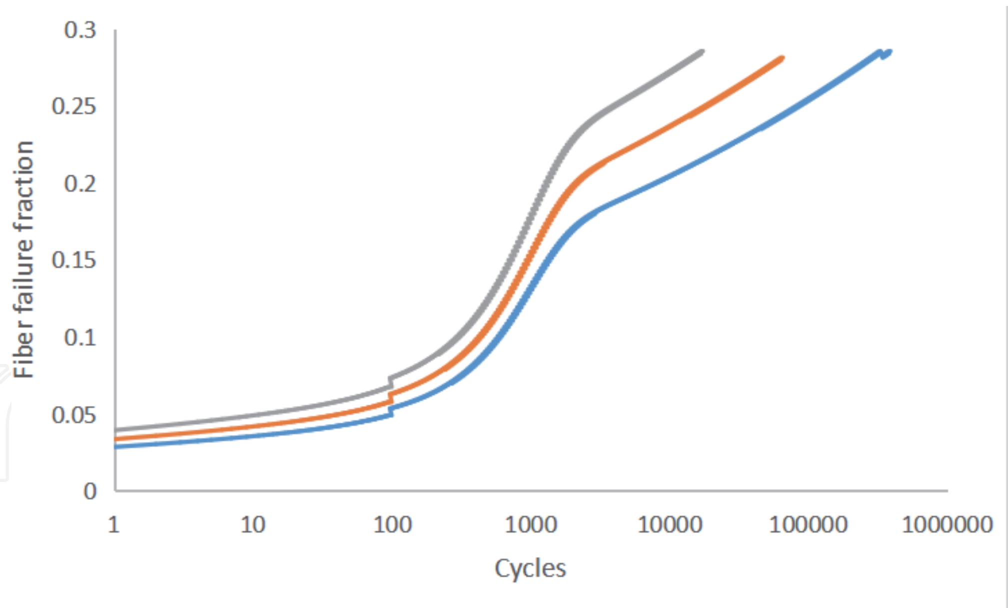

Figure 11.
The fiber failure fraction versus cycle number curves under different random stresses at N = 100.

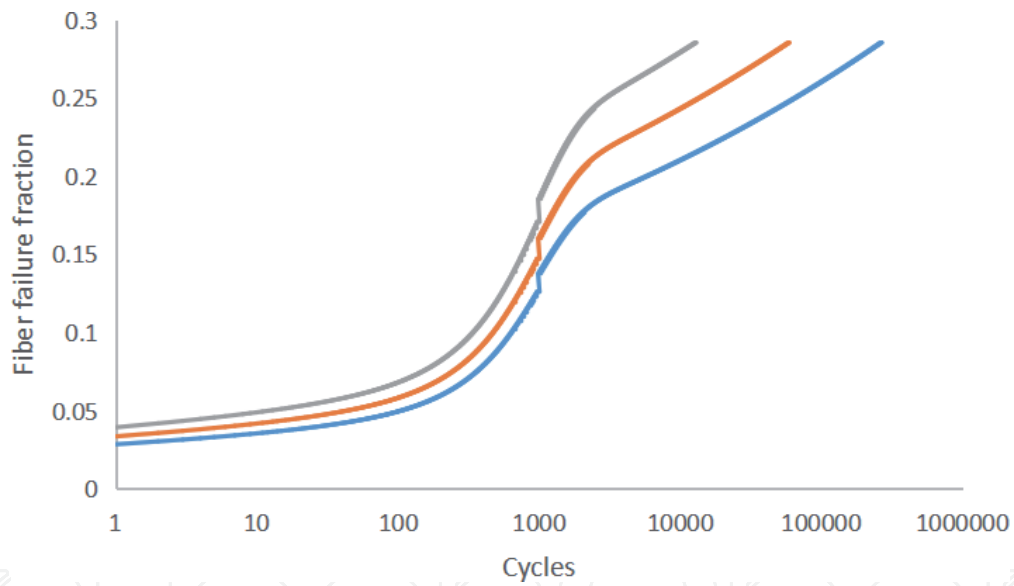

Figure 12.
The fiber failure fraction versus cycle number curves under different random stresses at N = 1000.

cycle, due to the random load of σ_s = 360 MPa, the fiber failure probability increases 0.015464 than the original value under σ_{max} = 355 MPa, the difference of fiber failure probability continues after 10,000 cycles, and the life is reduced from the original N = 389,642 cycles under σ_{max} = 355 MPa to N = 221,415 cycles, and the life difference is 168,227 cycles. The occurrence of random load reduces the fatigue life and decreases the fatigue life by 43.2% relative to the original value.

Table 1 shows the fatigue life and fiber failure fraction under σ_{max} = 355 MPa and random load of σ_s = 360 MPa at different cycle number. The difference of fiber failure probability under random load increases with the increase of cycle number. The long-term use of ceramic matrix composites with multiple cyclic loads has weak resistance to random loads and low safety and reliability, but on the contrary, the initial use of ceramic matrix composites has a strong ability to resist random loads and high safety and reliability.

3.2 Effect of random load peak stress on fatigue life

The parameters of C/SiC composite are as follows: p_1 = 0.01 and p_2 = 1.0; the interfacial shear stress parameters are ω = 0.04, λ = 1.5, τ_{i0} = 8 MPa, and τ_{imin} = 0.3 MPa; and the other parameters are given by V_f = 0.42, σ_c = 2 GPa, m = 5, and τ_i = 10 MPa. As shown in **Figures 11–13**, the random loads of σ_s = 360, 370, and 380 occur at the applied cycles of N = 100, 1000, and 10,000, and the percentage of fiber failure increases with peak stress and random stress. As shown in **Table 2**, the difference between the fiber failure fraction under constant peak stress and the fiber failure fraction under random load stress increases with the random stress level. As shown in **Table 3**, the difference of the cycle life decreases with the

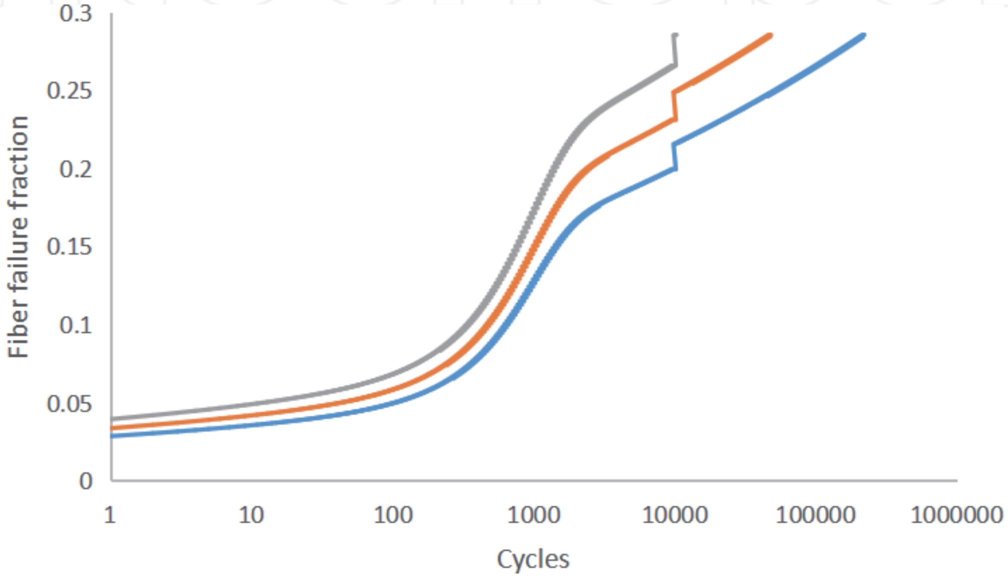

Figure 13.
The fiber failure fraction versus cycle number curves under different random stresses at N = 10,000.

Peak stress (MPa)	Fiber failure fraction difference at 100 cycles	Fiber failure fraction difference at 1000 cycles	Fiber failure fraction difference at 10000 cycles	Fatigue life difference at 100 cycles	Fatigue life difference at 1000 cycles	Fatigue life difference at 10000 cycles
355	0.004207	0.010321	0.015464	54,466	121,466	168,227
365	0.004784	0.011549	0.017028	14,888	32,234	43,591
375	0.005412	0.012827	0.012828	4008	8399	11,076

Table 2.
Comparison of fatigue life under different random stresses.

Peak stress (Mpa)	Decay rate of loading cycle in 100 cycles	Decay rate of loading cycle in 1000 cycles	Decay rate of loading cycle in 10,000 cycles
355	14.0%	31.1%	43.2%
365	16.2%	35.2%	47.5%
375	18.7%	39.7%	51.7%

Table 3.
Comparison of cyclic decay rates under different random stresses.

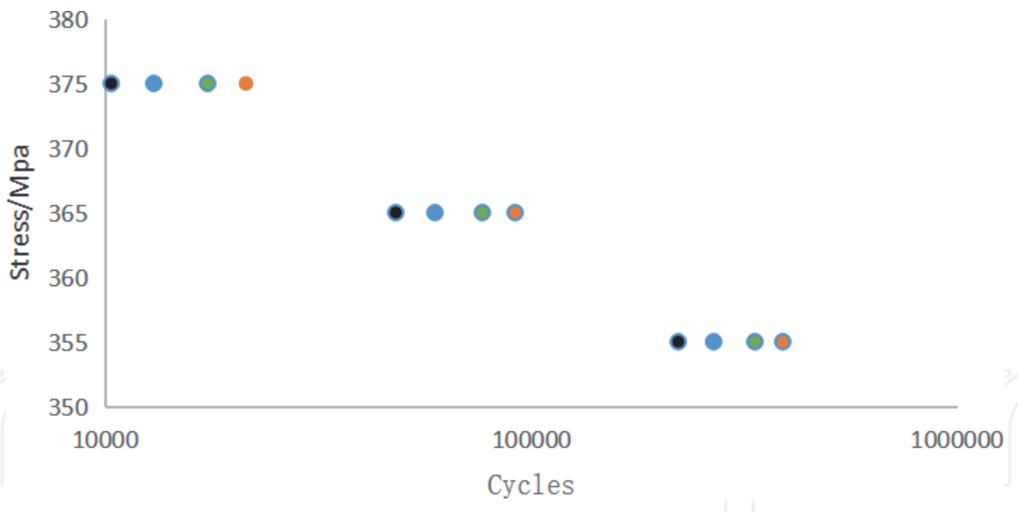

Figure 14.
The fatigue life S-N curve under different random stresses.

increase of the peak stress, the proportion of the reduced cycle to the total cycle increases, so the effect of the random load on the higher peak stress is greater. As shown in **Figure 14**, the fatigue life decreases at higher random stress.

4. Conclusion

The influence of random load on fatigue life of high-temperature ceramic matrix composites is investigated. A curve of fiber failure rate with cycle number and an S-N curve of fatigue life of C/SiC composites are presented in this paper. The random loads are loaded under different peak stresses, and the variation law of fiber failure rate and cycle life is analyzed. It can be concluded that when the same random load is added under the same peak stress, the difference of fiber failure rate increases with the increase of cycle number at which the random load occurs, and when the same random load is added at the same cycle number, the difference of fiber failure rate increases with the increase of peak stress. If the added random load is too high and exceeds the material's bearing limit, the fiber will break directly.

Author details

En-Zhong Zhang
College of Civil Aviation, Nanjing University of Aeronautics and Astronautics, China

*Address all correspondence to: 1913054374@qq.com

References

[1] Ma QG, Liu HT, Pan Y. Research progress on the application of C/Si C composites in scram jet. Journal of Inorganic Materials. 2013;**28**(3):247-255

[2] Sabelkin V, Mall S, Cook TS. Fatigue and creep behaviors of a SiC/SiC composite under combustion and laboratory environments. Journal of Composite Materials. 2016;**50**(16): 2145-2153

[3] Min JB, Xue D, Shi Y. Micromechanics modeling for fatigue damage analysis designed for fabric reinforced ceramic matrix composites. Composite Structures. 2014;**111**(1): 213-223

[4] Longbiao L. Damage monitor and life prediction of carbon fiber-reinforced ceramic-matrix composites at room and elevated temperatures using hysteresis dissipated energy-based damage parameter. Composite Interfaces. 2018; **25**(4):335-356

[5] Lee SS. Damage Analysis and Mechanical Response of as Received and Heat Treated Nicalon/CAS-2 Glass Ceramic Matrix Composites. Blacksburg, VA (United States): Virginia Polytechnic Inst. and State Univ.; 1993

[6] Evans AG, Zok FW, Mcmeeking RM. Fatigue of ceramic matrix composites. Acta Metallurgica et Materialia. 1995; **43**(3):859-875